



**HAL**  
open science

## Off-line correction method suitable for a machining robotapplication to composite materials

Guillaume Carriere, Mourad Benoussaad, Vincent Wagner, Gilles Dessein,  
Benjamin Boniface

### ► To cite this version:

Guillaume Carriere, Mourad Benoussaad, Vincent Wagner, Gilles Dessein, Benjamin Boniface. Off-line correction method suitable for a machining robotapplication to composite materials. International Journal of Advanced Manufacturing Technology, 2020, 110 (9-10), pp.2361-2375. 10.1007/s00170-020-05947-x . hal-03139191

**HAL Id: hal-03139191**

**<https://hal.science/hal-03139191>**

Submitted on 11 Feb 2021

**HAL** is a multi-disciplinary open access archive for the deposit and dissemination of scientific research documents, whether they are published or not. The documents may come from teaching and research institutions in France or abroad, or from public or private research centers.

L'archive ouverte pluridisciplinaire **HAL**, est destinée au dépôt et à la diffusion de documents scientifiques de niveau recherche, publiés ou non, émanant des établissements d'enseignement et de recherche français ou étrangers, des laboratoires publics ou privés.







OATAO is an open access repository that collects the work of Toulouse researchers and makes it freely available over the web where possible

This is an author's version published in: <http://oatao.univ-toulouse.fr/27369>

**Official URL:**

<https://doi.org/10.1007/s00170-020-05947-x>

**To cite this version:**

Carriere, Guillaume  and Benoussaad, Mourad  and Wagner, Vincent  and Dessenin, Gilles  and Boniface, Benjamin *Off-line correction method suitable for a machining robot application to composite materials*. (2020) *The International Journal of Advanced Manufacturing Technology*, 110 (9-10). 2361-2375. ISSN 0268-3768

Any correspondence concerning this service should be sent to the repository administrator: [tech-oatao@listes-diff.inp-toulouse.fr](mailto:tech-oatao@listes-diff.inp-toulouse.fr)

# Off-line correction method suitable for a machining robot application to composite materials

Guillaume Carriere<sup>1</sup> · Mourad Benoussaad<sup>1</sup> · Vincent Wagner<sup>1</sup> · Gilles Dessein<sup>1</sup> · Benjamin Boniface<sup>2</sup>

## Abstract

Robotic machining finds its place in a multitude of applications with increasingly restrictive dimensional tolerances. In the machining of left-handed shapes for the production of large composite supports (4-m diameter), the expected shape accuracy is a few hundredths. The industrial robot is not initially compatible with such performance criteria. The literature possesses several ways to improve the accuracy of industrial robots such as stiffness, or stress modeling with dynamic measurement of forces during machining. These methods are difficult to apply in an industrial context because they are too costly in terms of time and investments related to the identification means. This study proposes a new off-line correction based on the mirror correction applied during machining. This method is quickly applicable and required only a 3D vision system. Moreover, it is adapted to any 6-axis serial robot, unlike existing methods that requires a robot modeling and characterization, which is adapted to a specific robot only. After measuring the position of the tool during a first machining operation, this measurement is compared with the initial program setpoint for identify the robot deviation. A smart and autonomous process is used to re-edit the toolpath to compensate for the deviation. A new machining operation quantifies the correction by producing a part with improved shape tolerances. This article presents the development method, the implementation, and the results obtained following its industrial context. A gain of more than 80% is identified and an analysis of this result is proposed. Future complementary developments are suggested as perspectives.

**Keywords** Robotic machining · Composite machining · Robotic accuracy · Error compensation · Mirror correction method · Vision-based measurements

## Nomenclature

$V_c$  Cutting speed in m/min  
 $F_z$  Feed per revolution in mm/tooth

✉ Guillaume Carriere  
guillaume.carriere@enit.fr

Mourad Benoussaad  
mourad.benoussaad@enit.fr

Vincent Wagner  
vincent.wagner@enit.fr

Gilles Dessein  
gilles.dessein@enit.fr

Benjamin Boniface  
benjamin.boniface@groupe-lauak.com

<sup>1</sup> Laboratoire Génie de Production, Ecole Nationale d'Ingénieurs de Tarbes, Université de Toulouse, Tarbes Cedex, France

<sup>2</sup> Groupe LAUAK, LAUAK Innovative Solutions, Bagnères de Bigorre, France

COM method	Tool material pair method
$E_{C-track}$	Standard deviation of C-track device
$P_m$	Measured tool position
$P_i$	Desired tool position
$D$	Deviation between measured and desired tool position
$E$	Error vector
$E^*$	Correction vector
$P$	Measured tool position by C-track device
$P^*$	Correction tool position
CAM	Computer-aided manufacturing
CAM_p	Computer-aided manufacturing desired tool position
MES_p	Measured tool position by C-track device
RMS	Root mean square
$X_t, Y_t$	Effort measurement frame
$E_f$	Measured effort
<b>Eini</b>	Initial measured deviation by ATOS device

<b>Eatos</b>	Measured deviation after correction by ATOS device
<b>GYZ</b>	Calculate gain on the Y-Z sample plane

## 1 Introduction

Industrial robots can be found all over the world, in all types of industries, their number of integration increased by 19% in 2019 according to the IFR (International federation of robotics) [1]. Developed for pick and place and handling applications, the robot is increasingly being used for high-precision tasks such as machining or trimming. It represents 3% of the world's robotics park, and is destined to increase for coming years for some reason: Industrial robot is a flexible machine in addition to his lower investment compared with a 3 or 5-axis machine tool. It also has a larger working space with good operability. However, the kinematics of the serial robot is one of the main causes of his low rigidity for machining. The succession of joints and arms give this flexibility and do not allow it to perform movements with precision beyond some millimeters [2]. Regarding its repeatability, which is ten times smaller, it is possible to achieve better results by developing suitable correction methods.

The first studies aimed to improve the machining precision of a robot arm based on the measurement and modeling of stiffnesses. This fastidious method demands a long stiffness identification time and expensive means of measurement and analysis even though it proposes a gain of 50% of the initial accuracy of the means [3]. Its results depend on the quality of stiffness identification. Other methods added to this stiffness model, a robot calibration [4] or a stress model [5–7]. By increasing the number of phenomena taken into account in the positioning process, results were improved and the robot gained accuracy. The emergence of new measuring means, in these last years, has allowed the development of works on real-time correction by dynamic monitoring. The results are satisfactory since the accuracy achieved is close to a tenth of a millimeter [8–9] but they do not improve due to the processing time of the information and the measurement speed of the devices. All these methods are generally long and expensive. They are not adapted to the industry's needs, which require a robust method to be integrated into the robot's working environment.

Our study is a part of the composite materials machining field. The main difference between machining a conventional material and a composite material is due to the anisotropic construction of composite material [10]. The tool successively encounters two materials, the matrix and the reinforcement that have different machining properties. The matrix does not generate large cutting forces, but this polymer is sensitive to a thermal degradation. The reinforcement has generally a high Young's modulus, especially when it is a carbon based

reinforcement. Its important stiffness, resulting in high cutting forces, and it possess a very abrasive nature. These cutting forces variation on the tool edge, in addition to severe abrasive wear, makes difficult the material removal [11]. Studies have been made on optimum cutting conditions for composites. Abrão et al. [12] indicate that a low feed rate is more adapted to minimize the surface roughness criteria and that a high cutting speed allows the chip formation to occur as a fine particle which size of about 0.5  $\mu\text{m}$ . This minimizes cutting forces and improves tool life [13].

This work is in the area of robotic machining of large composite parts with a shape tolerance of less than a tenth of a millimeter. It is important to respond to the industrial need with elements applicable in this context. The advantage of this study is to not develop a long and tedious method of robot characterization nor a modification of its structure or design. This method is an off-line correction based on a trajectory measured by a 3D vision system, to improve the positioning accuracy of an industrial robot machining composite material parts. The originality of our work is to focus on developing a quick method adapted to any 6-axis robot and requires minimal experimentation, which is not the case with existing correction methods. The present paper proposes the off-line correction method adapted to the robot and based on the principle of mirror correction, which is already known in the world of machining. This method allows the machining of a complex part after the first step of process development. This tuning requires an external measuring means to determine the initial error of the robot. Then an autonomous process edits a corrected program that allows correcting the robot's inaccuracy in better proportions than precedent works.

The article is organized as follow. The next section presents first sources and causes of robot inaccuracy. In this section, we also introduce a preliminary test that has made it possible to define correction objectives. Section 3 described the off-line correction method. Then Section 4 introduces the experimental protocol, presents results of the correction, and discusses them. Then, conclusion and proposing perspectives of this work are summarized in Section 5.

## 2 Background

### 2.1 Sources of error in robotic machining

It is important to identify the different sources of error in robotic machining before proposing a new correction method. Precision machining refers to two capabilities, accuracy and repeatability. Accuracy characterizes the deviation of the position and orientation achieved from the truth or desired value. Repeatability refers to the ability of the device to repeat the same position, more or less precisely, for the same true value requested [3]. Among the criteria that define a machining

robot's performance, precision machining is probably the most consulted one when performing machining tasks. This criterion is a statistical data characterizing both the difference between average positions and orientations reached on the desired value and its dispersion [14]. The accuracy and repeatability values typically observed on industrial machining robots are about  $\pm 1$  mm and  $\pm 0.1$  mm respectively [15]. An analysis of the theoretical errors present in the work environment is presented in this section.

### 2.1.1 Robot-dependent errors

The machining precision of a robot is directly linked to its kinematic chain that connects the tool center point (TCP) to the ground. Its complex and multi-element construction and assembly make it more flexible than a 3-axis or 5-axis machine tool. There are two types of errors in the mechanical structure of the robot: geometrical errors, resulting from assembly or manufacturing errors of the robot components and are mostly linear regarding the parameters [16]. Often corrected by calibration, only the error due to gear's non-linearity is difficult to correct since it is a function of the robot's working space; non-geometric errors, which are also dependent on the task environment, are not corrected by calibration. They result not only from structural deformations of components, connections, and power transmission devices, but also from the robot component's wear. More generally, they are a function of the non-linear stiffness of the robot. According to Mustafa et al. [17], the flexibility of the links is responsible for 8 to 10% of the TCP position and orientation error. In addition to this static error, the flexibility of the joints causes a vibration of the structure when it is in motion. Variations in load and acceleration at the TCP generate visible resonance phenomena on its structures, which have low damping [18].

### 2.1.2 Process-dependent errors

In a robotic machining process, machining effort is the main source of position error. In aluminum milling, for example, these cutting forces can reach hundreds of Newtons and lead to 1-mm error according to Zhang et al. [19]. This cutting force value depends on the parameters; spindle speed, cutting depth, and cutting width, which determines a material removal rate and a specific cutting force. Some works study variations on the cutting force and chatter phenomenon which is extremely harmful to the quality of the machined surface [20].

Thus, several types of errors occur in the robotic machining context and several methods exist to correct them according to their origin. Section 3 details the method implemented in this study, which has the advantage of correcting all the errors mentioned above since it corrects the deviation measured to the end's robot.

## 2.2 Working environment

### 2.2.1 Context and limitations

The target application is surfacing of self-stiffening composite molds made of carbon fiber/epoxy composites. The reinforcement used in this assembly is a high-performance composite reinforcement named "48600 U 1250." This carbon fiber twill fabric (50% warp, 50% weft) has a nominal weight of 600 g/m<sup>2</sup> and a thickness of 0.62 mm. The resin and its hardener are respectively "HTG 240" and "HTG 245." This epoxy system is dedicated to the realization of structural composite parts with demanding TG up to 240 °C. Its mechanical characteristics are Young's modulus of  $E = 67,900$  MPa, a shear modulus of  $G = 6240$  MPa, and a Poisson's ratio of  $\nu = 0.3$ . This highly resistant material is characterized by an ultimate tensile strength of 750 MPa in the tensile test. These properties are useful when searching for information concerning the choice of tools adapted to the machining of this material. However, they do not influence the correction method developed here because this method applies to the measurement of the deviations observed at the robot's end device whatever the material being machined.

A previous study has defined tools and cutting parameters for each operation (Table 1). Various studies suggest interesting results concerning the tool's geometries to be privileged for the composite machining. It appears that the rhombic milling cutter geometry ensures a good quality of cut, and it has a disastrous cutting edge and a dextral cutting edge on each rhombic tooth, which can prevent defects such as tear and burr on upper surfaces of the workpiece [21]. The use of diamond-coated tools is also often favored, even in front of more expensive polycrystalline (PCD) tools [22]. We chose a diamond-coated rhombic milling cutter with a diameter of 10 mm for roughing operation and a spherical milling cutter with a diamond coating and two teeth for finishing operation, also in 10-mm diameter. The literature also shows that the sharpness of the cutting edge must be as fine as possible to ensure a clean break of the fiber [23], since it helps to minimize cutting forces and ensures good surface quality. The coating increases this value, and our roughing and finishing tools have edge radius values of 24  $\mu$ m and 15  $\mu$ m respectively. The application of a tool material pair method (COM method) on a CNC machine made it possible to identify them. This method is based on the hypothesis that the optimum depends on the set of cutting parameters ( $V_c, F_z, \dots$ ) which produces minimum specific energy (power/flow rate) during machining [24]. It defines the type of tool geometry for the machining sequence. In this research, tools and tool holders are considered infinitely stiff compared with the robot's rigidity.

The part is a circular part with a parabolic warped surface (Fig. 4) produced by the infusion process. The porosity rate provided by this process is less than 1.5% but it has the

**Table 1** Machining parameters

Milling	Tool	Vc (m/min)	N (tr/min)	f (mm/th)	Vf (mm/min)	ae(mm)	Ø(mm)	Teeth
Roughing	Diamond-coated carbide end mill	135	4300	0.2	1720	5.25	10	7
Finishing	Diamond-coated carbide ball end mill	180	5750	0.14	1605	0.346	10	2

disadvantage of leaving discontinuous raw surfaces in terms of material thickness. Therefore, a first machining will be carried out to reduce this thickness variation as much as possible. The COM method working in iso-thickness for the tool pass depth and also in iso-engagement will guarantee a constant cutting force. The machining sequence includes one roughing and one finishing operation. The literature attributes to this material an important abrasive character. The choice of cutting parameters is decisive to ensure surface quality and tool life [21]. Generally, polycrystalline diamond (PCD) and diamond-coated tools are preferred in composites machining. These tools can maintain a sharp cutting edge and reduce surface defects due to their high hardness.

### 2.2.2 Experimental study means

This study is carried out in a workshop consisting of a Kuka KR360 robot associated with a rotary table (Fig. 1) and controlled by a Siemens 840D controller.

The C-track from Creaform, a robust position sensor, is an optical CMM with a dual camera sensor. This system respects a measuring accuracy of  $\pm 0.15$  mm [25]. C-track can be integrated into a workshop with few limitations even optical disturbance such as carbon particle or water projections. That is why this device remains an asserted choice to respond to the context. A statistical study allowed us to identify a standard deviation of  $Et_{C-track} = 0.05$  mm. This parameter helps to implement a smoothing of its data in Section 3.3.3.

To validate the method and C-track's smoothing, a high-resolution scanner and a measurement column are used (Figs.

1 and 2). The ATOS triple scan product provides three-dimensional measurement data accurate to 0.05 mm [26] and the HC3 measurement column gives measures with a micron resolution and a maximal measure error to 3  $\mu$ m.

### 2.3 Preliminary test

First dynamic monitoring of machining on the material allows useful observations to establish a machining strategy. These are plane machining operations with standard cutting parameters. The measured tool position ( $P_m$ ) is used to determine deviations ( $D$ ) on X and Y (Fig. 3) of the robot from the desired position ( $P_i$ ) such as Eq. 1:

$$D = P_i - P_m \quad (1)$$

Figure 3 correlates the X and Y coordinates of the moving tool with the calculated deviations on the same axis relative to time. The tool makes an out-of-matter movement to approach the part before the machining phase (rectilinear path carried by the X axis), the beginning of which is represented by a green vertical line (Fig. 3).

As the tool moves, variations in tool deflection are observed in each of the two shown axes. Firstly, each change of direction causes a significant deviation of 0.5 mm. As soon as the path of an axis changes rapidly (vertical red lines), a deviation appears (red arrows). Its rapid evolution on a trajectory leads to changes in the dynamic behavior of the robot. For the observed direction changes, the articulations of the robot

**Fig. 1** From left to right, Kuka KR360 robot and its rotary table, C-track, and ATOS

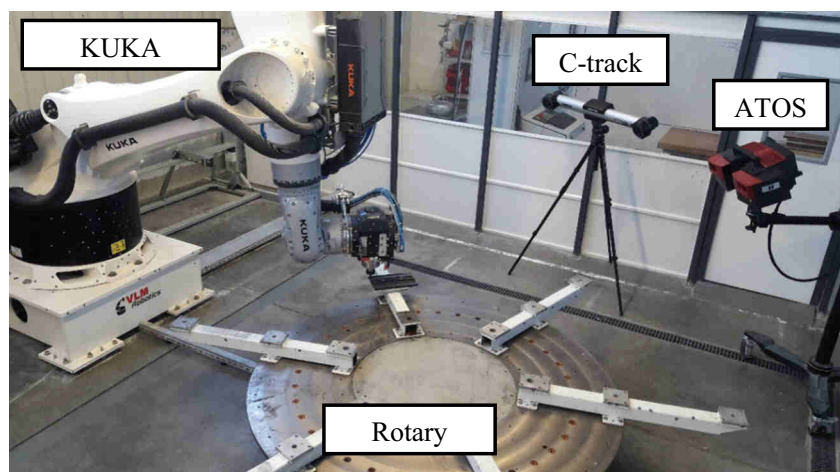


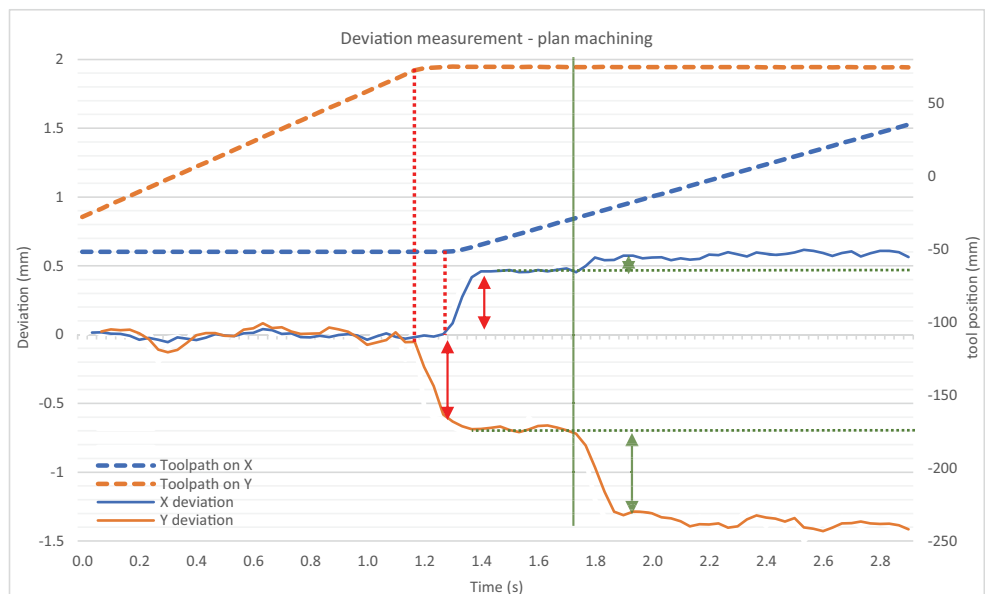


Fig. 2 Measurement

base and arms 1 and 2 modify their accelerations to follow the trajectory of the tool. In the first part of the movement (before the first vertical red line), robot base has a high speed of movement in front of the other two. In the second part (after the second vertical red line), it is the opposite. Its variations in speed and acceleration highlight the backlash and flexibility of joints. A phenomenon called inversion [7] identifies the case where a joint goes from a rotation in one direction to its opposite direction. The consequences in terms of deviations are similar or even greater.

Secondly, the tool enters into contact with material and immediately generates a deflection in both axes shown (green

Fig. 3 First measured machining



arrows). Without machining, robot structure is only subject to gravity and its own weight. But as soon as tool-material interaction generates cutting forces to compensate material deformation and material removal, these new interactions disturb positioning. Elements of the robot will transmit these forces to its base and the bending of each component characterized by its stiffness explains the deflection of the final organ.

From a machining point of view, the robot's deviations are carried out logically. This is because the robot deflects in the opposite direction to the machining force vector. Force measurements on a load plate allow measuring the components of the cutting force. It turns out that the force carried by the Y axis is almost three times greater than that carried by the X axis. This justifies a greater deviation of the robot on the Y axis. On the other hand, the direction of the deviations is also consistent with the strategy of the machining pass, i.e., machining with half the tool engaged axially in the positive direction X. To respect this eventuality, it must be added that robot stiffness in the X and Y directions are considered to be relatively close.

These initial measurements made it possible to highlight the two main causes and impacts on tool deviation that occur during machining, inversion and cutting forces. The first contribution of the following method lies in the correction of a measured deviation from several different sources without precise characterizations of this error sum. The second is the anticipation of inversion phenomena to confer to the corrected program a better dynamic approach to its regions.

## 2.4 Machining strategy

Most composite machining applications involve routing operations where it is regularly claimed that conventional

machining give better surface roughness [27]. It also appears that reinforcement orientation determines the machining quality, the cutting force intensity, and the appearance of defects such as delamination, chipping, or burrs. These defects are important and feared in composite material machining [28]. In 5-axis surfacing, Morandea et al. [29] draw the same observations. He concludes that it is necessary, as much as technically possible, to orientate the cutting speed axis and the fiber axis with an angle of  $45^\circ$  or  $90^\circ$  and to avoid  $0^\circ$  and  $135^\circ$  angles, because it minimizes axial forces that lead to a severe wear in clearance by the elastic return of the fiber on the clearance face of the tool. In our case, since we do not know the fiber orientation plan, because it is a random tissue positioning fabrication, we could not apply these rules.

Regarding part's geometry, it is chosen to use the potential of the dividing plate present in the cell and implement a spiral machining strategy on the X, Y plane (Fig. 4), to limit the inversion phenomena if the robot must turn around the part center. The table ensures the feed speed of the tool and the robot performs the radial feed. The robot describes a straight path to machine from the end of the workpiece to its center like a turning strategy.

### 3 Off-line correction

#### 3.1 Principle of mirror correction

There are two types of toolpath correction, an offline correction and an on-line correction. The offline correction is a correction that is made before the machining phase, while the on-line correction is made during the machining phase. The offline correction is generally used due to its analysis and data processing time, and also by using sensors with significant acquisition and response times. In his article, Schneider et al. [9] use both types of correction, where off-line correction is based on the kinematic and dynamic simulation and on a stress model. On-line correction based on tracking measurements.

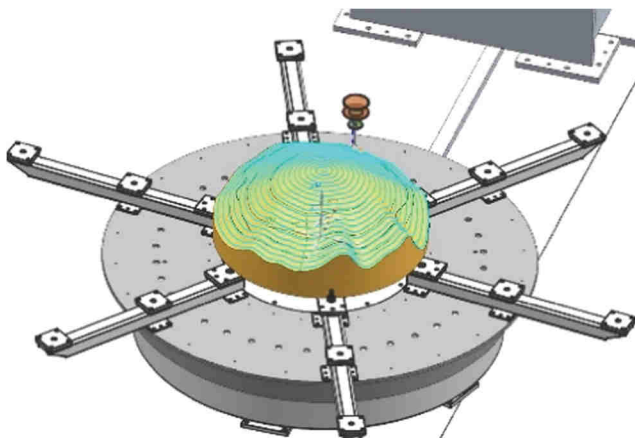


Fig. 4 Spiral machining strategy

He concludes that it is difficult to use both approaches because of time synchronization's problem of the two corrections. He also concluded that feedback loops would need to be further improved to claim a high performance of on-line correction and that external sensors are currently the limit of this method. To meet our objectives without heavy and sophisticated equipment that can be integrated into an industrial work environment, it is not possible to perform an on-line correction. Therefore, off-line correction is chosen in this paper.

The method used is based on the mirror correction principle. This type of correction is used in the world of machining because it is a reliable and robust method. Olabi et al. [30], in their work, clearly explain how mirror correction works. The method is based on measurements only. During machining, a measurement of the tool's coordinates (measured path) is recorded and compared with the originally planned path (desired path). Figure 5 shows a series of points that symbolize the actual toolpath that does not match with the desired toolpath. The principle is to generate a compensated path by adding a normal correction vector ( $\mathcal{E}^*$ ) to the desired path at any measuring point. This correction vector is equal to the norm and opposite to the direction of the error vector ( $\mathcal{E}$ ). The error vector is the normal distance between the desired path and the measured path. This compensated path is used for re-machining, which corrects the positioning error. Other works [31–33] have since worked on improving the correction by using parametric curves such as B-spline or NURBS. The aim is to remove or smooth out as much as possible the part of the measurement error in the correction.

In the studies mentioned above, mirror compensation is used on CNC machine tools to correct mechanical slack in the translation axis's links or deviations resulting from high cutting forces. These machines are extremely rigid, so the error displacement value is close to a few microns meters [23]. Robot's measured error is about  $\pm 1$  mm (Fig. 3). The robot's stiffness is variable and depends on its posture [4]. A hypothesis of this study is to neglect this variation of stiffness in a circle of 2-mm diameter around the measured tool position and for the same applied force. It is then supposed that the robot behavior at a measured point remains identical to its corrected point.

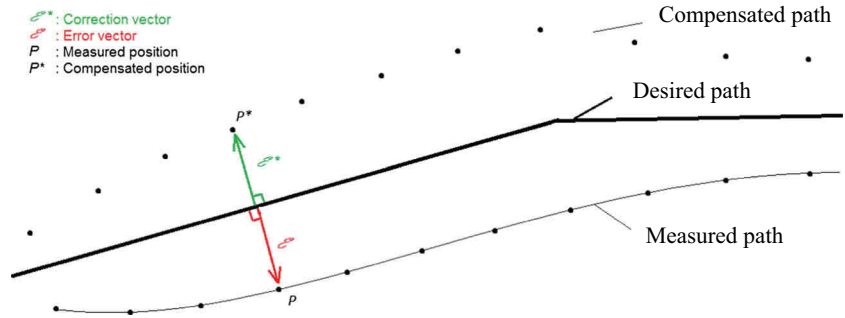
#### 3.2 The correction protocol

The correction protocol presented here is reproduced at each step of the machining process, roughing, semi-finishing, and finishing.

This correction consists of five stages: First machining operation with measurement of tool path, error analysis by the correction process, corrected path generation, second machining measuring tool path, part analysis, and correction gain.



Fig. 5 Mirror correction method



1. The first machining operation is the experimentation of the path. The robot control executes the numerical control (NC) program for the desired path. The real path is measured and saved by the dynamic tracking system before correction.
2. The correction process performs the analysis and processing of NC programs and C-track measurement data. The result of this step is a continuous deviation as a function of time between both.
3. Generate the correction path consists in the calculation of the corrected path according to the desired path and the continuous deviation.
4. Second machining operation is the experimentation of the corrected path. The robot control executes the NC program of the corrected path and the dynamic tracking of the real path after correction is monitored.
5. Correction gain analysis is determined by analysis of several data. The new deviation is not only found during the second machining operation, but also by measuring the machined surface with two sensors: one non-contact sensor, ATOS, and one contact sensor, HC3 column measurement.

Steps 2 and 3 are realized by an autonomous process developed as follows.

### 3.3 Intelligent and autonomous correction process

As a post-processor, this procedure is a succession of analyses and calculations of input data in order to propose a corrected program adapted to robotized machining. It is based on statistical and physical criteria which are detailed in this section: time synchronization of input data, calculation of tool positioning error, smoothing error according to criteria, and generation of the corrected toolpath.

#### 3.3.1 Input data synchronization

The correction principle is carried out axis by axis as shown in Fig. 6, where a schematic example of a Cartesian axis is presented. The CAM software generates an ISO format program. NC program is a succession of controlled points with 3

Cartesian coordinates, 3 orientation coordinates and tools feed speed information. These data in position and displacement speed permit to deduce the desired path (CAM\_p). The C-track measuring device gives the real measured path (MES\_p) as a succession of points (X, Y, Z translation components and A, B, C rotation components). Its points are described over time with a measuring frequency of 30 Hz.

These two signals such as (CAM\_p) and (MES\_p) are synchronized using a 2-s pause in the NC program. After that, first function of the correction process is to reconstruct the continuity of the desired path. The transition from one point to the next is carried out in a straight line (Fig. 6) as controlled by the program by means of linear interpolation (G1). This recreated interpolation makes it possible to determine the desired position for any time, in particular those corresponding to the C-track measuring points.

#### 3.3.2 Deviation error

Comparing measured and desired position, a deviation is obtained (red arrow Fig. 6) which is referred to the error vector ( $\mathcal{E}$ ). Contrary to the principle of mirror correction explained above, this error vector ( $\mathcal{E}$ ) is not normal to the desired trajectory but is normal to the time axis. Figure 6 shows that for a measured point  $P$ , the associate corrected point  $P^*$  is such that Eq. 2:

$$P^* = P - \mathcal{E} \quad (2)$$

With:  $\mathcal{E} = \text{MES}_p - \text{CAM}_p$

Also represented on Fig. 6 are measured points in red and their corrected point in green. This step allows calculating the error vector ( $\mathcal{E}$ ) over time, essential for further data processing.

#### 3.3.3 Smoothing of calculated deviation

Figure 7 shows the of deviation error calculation on Y axis (tool feed rate axis) for 12 machining seconds. C-track measurement noise leads to variability in the calculation of the deviation. Not to apply a correction deviation that can be up to 0.2 mm between two consecutive measured points, smoothing is necessary, and is based on the filtering of signals. This

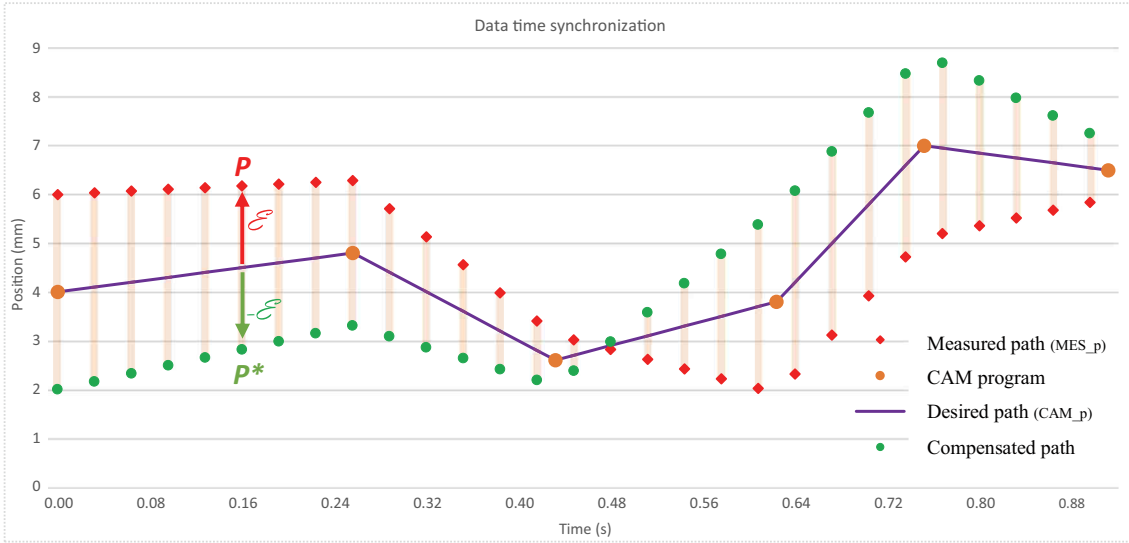


Fig. 6 Schematics of correction process operations

smooth showed respect criteria to propose a correction that considers as much as possible the measured physical phenomenon.

Developed smoothing consists of cutting the measured sequence by zones and identifying a linear regression by zone. The choice of the zone's number is governed by a constrained statistical iteration procedure. The first condition to be met is that a minimum of  $n = 40$  measurement points per regression must be maintained. This number of points determines a "smoother" aspect of the measurement. This choice is the result of a bias-variance compromise [34], and the minimization of the root mean square (RMS) criterion. RMS is the arithmetic

mean of the squares of a set number and its mathematically calculated as Eq. 3:

$$\text{RMS}_{\text{regression}} = \sqrt{\frac{1}{n}(\epsilon_1^2 + \epsilon_2^2 + \dots + \epsilon_n^2)}. \quad (3)$$

The C-track measuring accuracy has a normal distribution and its standard deviation is given by  $\text{Et}_{\text{C-track}} = 0.05$  mm. The linear regression which tends to limit the signal fluctuations must not limit the information of the measurement. To ensure that, RMS value is regarding:

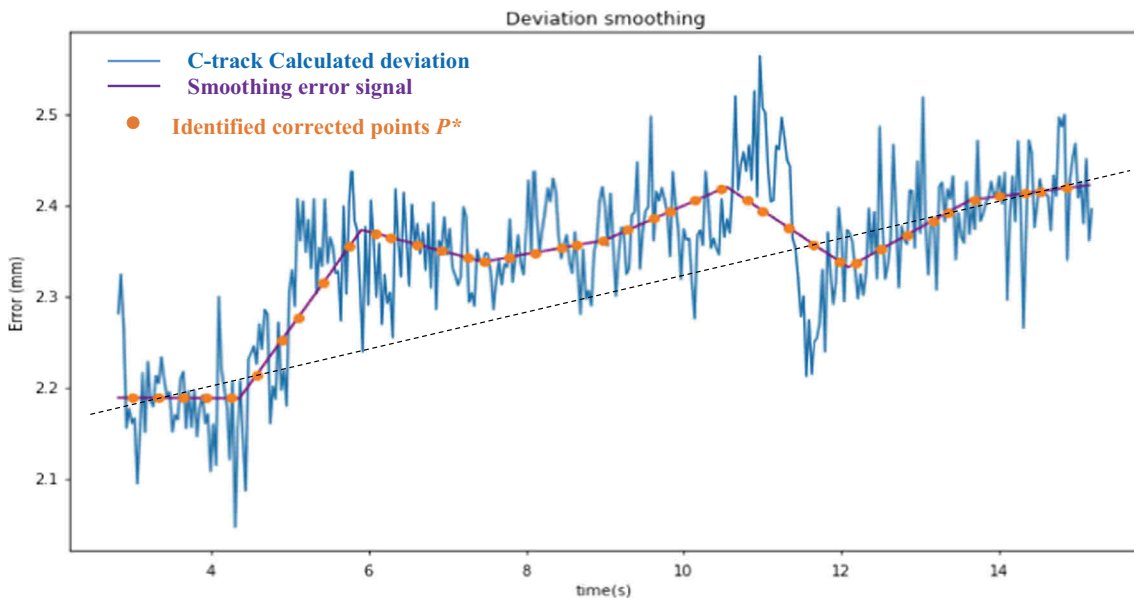


Fig. 7 Measurement processing

- $RMS_{\text{regression}} \gg Et_{C\_track}$  means that gaps between C-track measurement and regression are much too wide and regression is not representative to the real path.
- $RMS_{\text{regression}} = Et_{C\_track} \pm 0.01$  means that gaps are similar to C-track measurement gaps. The smoothing is representative of the real path.
- $RMS_{\text{regression}} \ll Et_{C\_track}$  is impossible because the C-track's standard deviation is the restrictive parameter of the regression's performance.

Based on twelve similar machining toolpaths, a convergence study of these two criteria by changing the size of the smoothing zones is presented (Fig. 8). For this machining example, cutting into 8 smoothing zones makes possible to keep a sufficient number of measurement points per regression while minimizing the RMS criterion. That ensure a minimum lost of information from the raw signal.

This smoothing method (Fig. 7) limits the variability between two measured points to be corrected. It ensures a filtering of the measurement noise while keeping the maximum information on the real position of the tool. Consequently, it also minimizes variations between two points of the corrected program. The robot's position is then corrected smoothly and continuously.

### 3.3.4 Program correction

According to this deviation smoothing, each measured point has a new corrected point represented by the purple line in Fig. 7. The initial NC program has 40 points when the number of measured points by the C-track is 370. The corrected program would have much more points than the initial program and it would change the dynamic response of the robot, which is to be avoided. The choice is therefore to keep the same number of crossing points. Deviations values are identified on the smoothing error signal, purple line in Fig. 7, according to time's desired points of the NC program. Consequently, there are corrected points  $P^*$  (orange points on Fig. 7) for each desired point as follows.

It processes each coordinate separately and applies a 6-coordinate compensation vector to each point of the original program. The corrected program is now edited in ISO format preserving the program header and end, the feed, and rotation characteristics of the tool.

The last part consists in executing this corrected path, tracking tool position, and measuring the workpiece surface to characterize benefits of the method.

## 4 Results and discussions

The validation is done on samples of the composite material with a toolpath part of the application one. It represents about thirteen machining minutes. Only one result is graphically depicted but performance indicators are based on ten measurements.

As presented in Fig. 9, the material sample is fixed on the rotative plate. The robot end-effector movement is described on the Y-Z plan for an X coordinate  $x = 0$ . Tool executes a part of the spiral strategy during the machining. Only the machining part of the toolpath is considered in the correction method. The robot's deviations observed when the tool is out of the material is therefore not taken into account and uncorrected.

During the COM method mentioned in Section 2.2.1, cutting forces were recorded to find the optimized cutting parameters. Knowledge of its efforts helps to analyses the correction results. The  $(X_t)$  and  $(Y_t)$  vectors in Fig. 9 represent results of the cutting force applied to the tool for values of 46 N and 90 N respectively on the X and Y axes of a reference frame tangent to the path (red frame). The force vector (E), which is the combination of its resultant values, is therefore 101 N in the X-Y plane. The direction of this cutting force implies, in the measuring frame (orange frame), a higher deviation on the Y axis compared with the X axis. For this reason, the following detailed results relate to Y axis compensation. Conclusions consider the correction in the three axes and the three orientations.

Fig. 8 Statistical iteration procedure—Y axis example

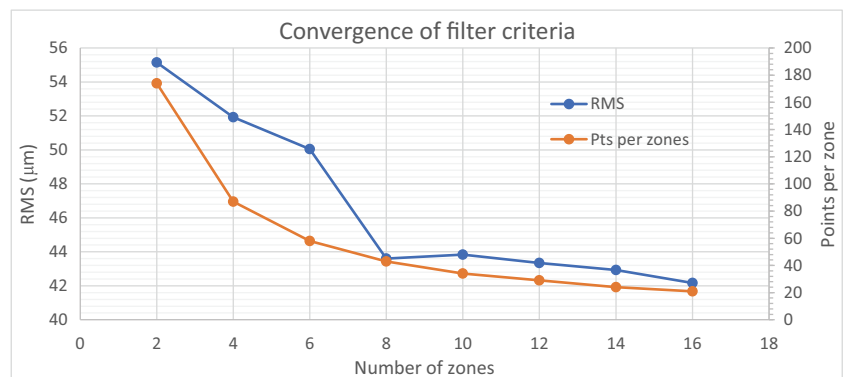
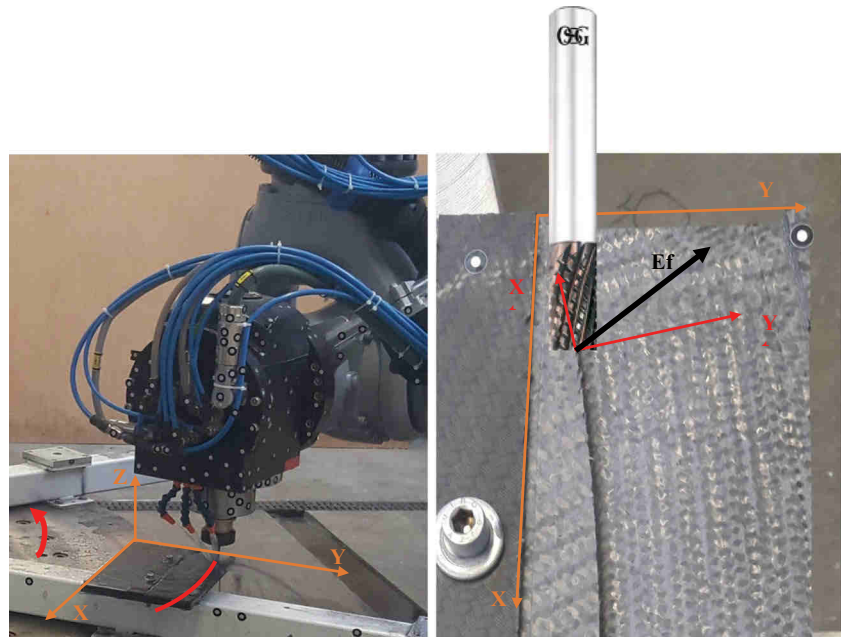


Fig. 9 Robot trajectory definition



#### 4.1 Deviation and corrected program analysis

Figure 7 shows all the correction procedures applied on the Y axis measurement which is the most representative axis of the robot's positioning error. The deviation evolves between 2.2 mm and 2.4 mm, a significative error of many sources. Machining forces are the main reason for its deviation. The dashed line present on Fig. 7 indicates that another source of error is present since the engagement of the tool in the material is constant and therefore the cutting force is constant as well. This deviation is caused by the sum of probing inaccuracies of the robot and the tracking mean taking the workpiece data, which add a bias to the tool position measurement.

For this calculated position error, the smoothing iterative procedure is released into 8 zones (Fig. 8) with a minimized  $RMS_{\text{regression}} = 0.052$  mm and a number of measured points per regression  $n > 46$ . The identified orange points are representing deviation values for correction of the CAM program.

#### 4.2 Correction analysis

First analysis is the machining time of the corrected toolpath: 12,968 min compared with 12,964 min for the initial program.

The machining time is not extended, it means that the trajectory modification is small and chosen criteria are therefore quite limiting to guarantee such results. A succession of 10 machining operations are carried out in the specimen.

Figures 10, 11, and 12 show the tool positioning error over time during machining to one pass (the 8th path Fig. 13), before and after the correction respectively for the measured X, Y, and Z axes of a same toolpath. Table 2 shows the performance indicators before and after the correction method. Its criteria from the C-track measurement provide additional information for the analysis of this correction. These are the measured average deviations and the calculated RMS. Its criteria are verified in the following section with the use of other means of measurement to characterize the correction.

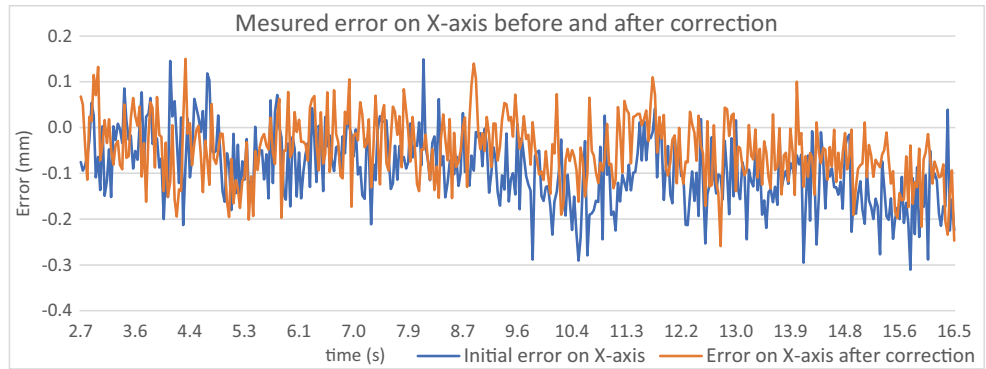
Figure 10 shows that the corrected toolpath improves about 50% the accuracy of tool position on the X axis. Indicators in Table 2 confirm this finding with a decrease in mean error and RMS of 40  $\mu\text{m}$ . Measurement noise remains similar to the two measurements, oscillating by one value of the measurement uncertainty around the mean value.

As regards of the trajectory on the Y axis, the improvement is more important (Figure 11). Indicators justify an improvement of 2 mm in the mean error, and RMS criterion shows a same evolution. On this axis, a change in the evolution of the

Table 2 Performance indicators on 10 machining paths

(mm)	Before correction				After correction			
	X	Y	Z	Vector	X	Y	Z	Vector
Mean error	- 0.084	2.340	0.828	2484	- 0.043	0.323	0.049	0.329
RMS (error signal)	0.113	2.342	0.836	-	0.081	0.337	0.104	-

**Fig. 10** Error measured on first and second machining—X axis



positioning error during machining is observed. Initially increasing from the beginning to the end of the measurement, after correction, the error is decreasing. The tool moves out of the material of 2017 mm, difference between initial and corrected measurements (Fig. 11). The engagement of the tool is therefore less important, and the cutting forces decrease modifying the reaction of the robot's structure. In this case, the considered linear response domain of the robot is not known and shows a limit of the method. For this reason, the mean residual error is 0.32 mm (Table 2).

Likewise, correction is beneficial for the Z axis path. Table 2 shows a gain of about 0.8 mm for the RMS and mean error values. This error measured after correction oscillates around zero (Fig. 12). However, two peaks are observed and identified for values about  $-0.2$  mm and  $+0.2$  mm. To explain its measured defects, the Z trajectory is shown in red on the same graph. This trajectory describes two extremes, first with a value of  $+5$  mm on the axis and the second for  $-7.7$  mm reached at 5.1 s and 11.6 s respectively. Figure 12 clearly shows the link between its path changes and the measured error peaks that appear at the same machining time. This correlation makes it possible to attribute its faults as the consequence of a change of path and an inversion of the evolution direction of one or more joints of the robot.

Two reversal faults are shown here, as described in Section 2.3. Its defects are also measured on the initial trajectory and are taken into account by the correction, but modifying the program does not make the system able to consider this

phenomenon and correcting it. Inversion is a structural phenomenon that can be solved or attenuated only with a dynamic study like a variable jerk command [35]. The same faults also appear on the measured errors of the X and Y axes (Figs. 11 and 12) for similar time values, i.e., 5.1 s and 11.6 s. For example, the faults found are about 0.1 mm and 0.2 mm for  $t = 11.6$  s, respectively, for the X and Y axes. That is to say that its inversions impact the positioning on the three axes X, Y, and Z.

As a reminder in Section 3.1, the robot stiffness behavior is considered linear with respect to initially measured errors, i.e., mean error vector = 2.5 mm (Table 2) for constant external loads. The correction modifies the interaction of tool in material since about 80% of the measured errors are corrected. Tool generates less material removal and forces applied after correction are less important and modify the initially measured response of the robot. Although robot stiffness behavior is linear and proportional to external forces applied to its structure, changing these interactions changes the bending of the robot and therefore the initially measured error is not fully corrected.

### 4.3 Experimental validation

A high-precision non-contact 3D scanner (ATOS) and a measurement column are used to make a comparison between C-track measurements and the machined surface to validate correction results. ATOS generates a point cloud of the workpiece

**Fig. 11** Error measured on first and second machining—Y axis

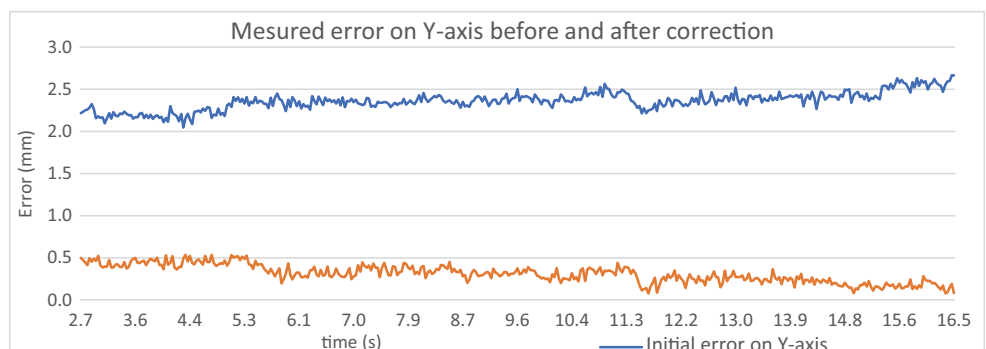
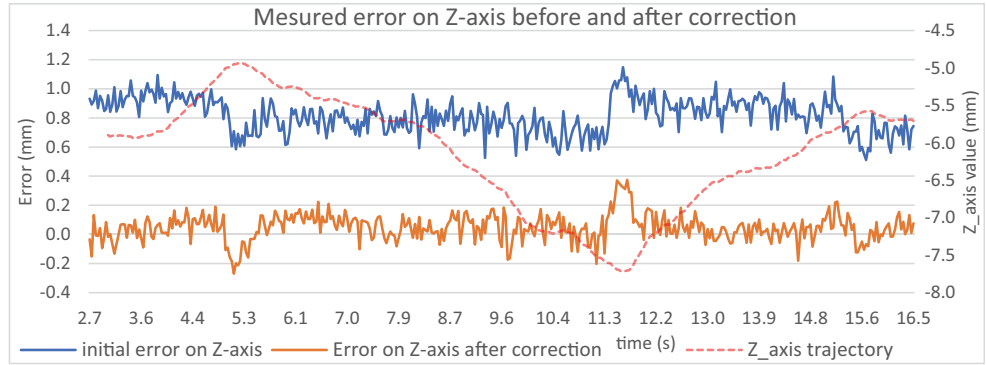


**Fig. 12** Error measured on first and second machining—Z axis



after machining and gives information about the geometry workpiece. The measurement column gives dimensions about palpated references.

Due to the machining procedure, it is possible to locally measure a deviation between the two machining operations (before and after correction) on both Y and Z axes. The correction values along the Y axis is measured in Figs. 13 and 14. The Z gap is determined by measuring the distance between the lower plane of the specimen and the residual material after the tool has passed through (Fig. 15).

Figures 13 and 14 show the measurements of both checking fixtures and the difference between the measured values. Table 3 details results and makes a comparison with the C-track measurements.

An average error of 0.025 mm is found between same measured dimension by measuring devices of this section. This observation allows interpreting the ATOS means as being able to qualify the correction in front of the C-track accuracy. Table 3 shows a difference of nearly 0.03 mm and 0.1 mm between the gaps found by its two means respectively on the Y and Z axes. Inaccuracy of the C-track's reference frame is part of this observed difference.

Considering the initial deviations determined by the dynamic monitoring of the first machining operation (**Eini**) and those measured by ATOS after correction (**Eatos**), it is possible to determine the correction gain in the Y-Z plane (**GYZ**) as Eq. 4:

$$GYZ = 1 - \frac{EatosYZ}{EiniYZ} \times 100 \quad (4)$$

**EiniYZ** is the error norm vector measured at the first milling and **EatosYZ** is the error norm vector by plane Y-Z measured by ATOS devices after correction as Eqs. 5 and 6:

$$EiniYZ = \sqrt{EiniY^2 + EiniZ^2} \quad (5)$$

$$EatosYZ = \sqrt{EatosY^2 + EatosZ^2} \quad (6)$$

Gain is expressed as a comparison between error vector norms before and after correction, it is a percentage based on the initial deviation. In this case, **GYZ** = 96.3% in the Y-Z plane.

The dynamic tracking performed by C-track gives results close to those observed with a scanner and a high-precision

**Fig. 13** Comparison ATOS and column measurement on Y after correction

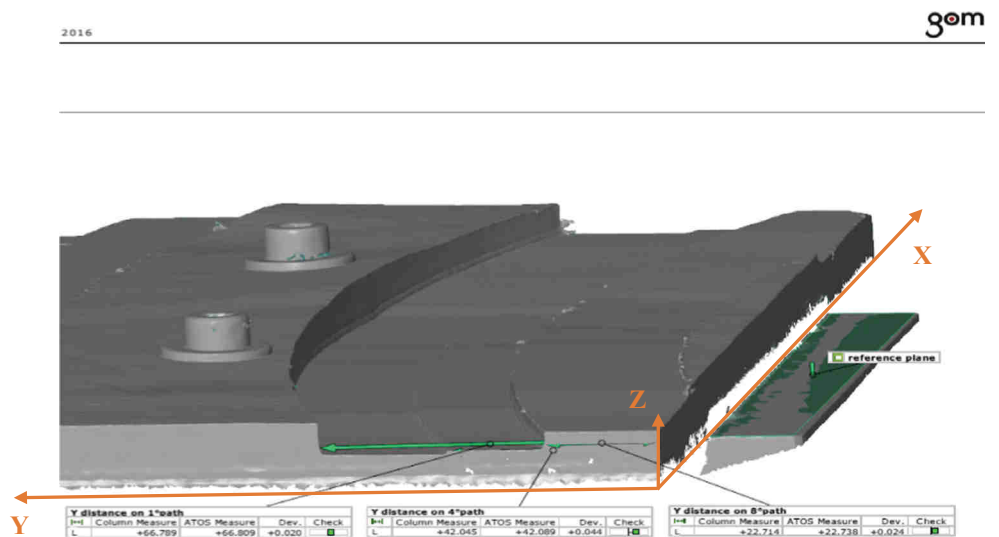
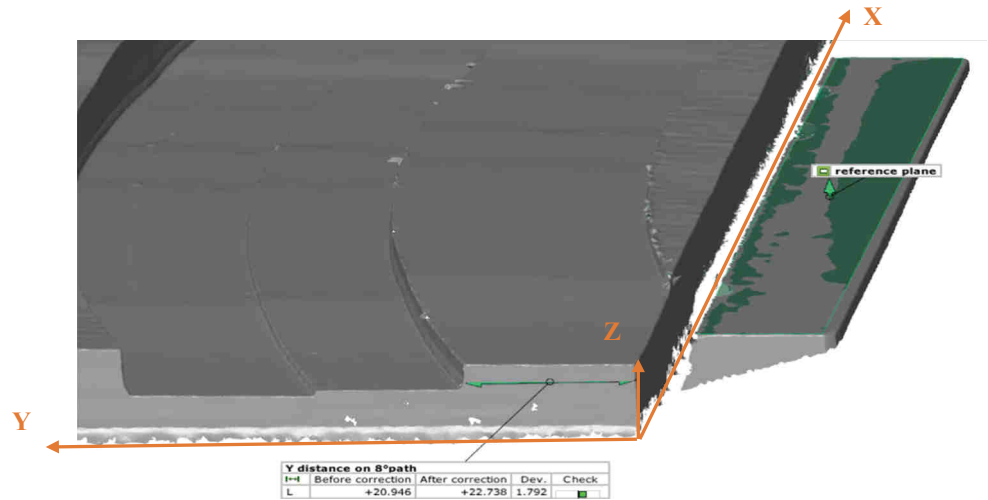


Fig. 14 ATOS measurement on Y axis



column measurement. Considering ATOS and C-track measurements on Table 3, deviations of 0.026 mm and 0.106 mm are calculated respectively on the Y and Z axes. On the YZ plane, the maximum vector error is equal to 0.109 mm. Then a measurement uncertainty of  $\pm 0.109$  mm can be cumulated to the C-track measurements. According to Table 2, the mean vector initially determined by the C-track is therefore  $2.484 \pm 0.109$  mm and after correction about  $0.329 \pm 0.109$  mm.

By studying the correction's potential in its high and low values of its error vectors, our correction method improves the positioning accuracy of the robot by  $87 \pm 5\%$ .

## 5 Discussion

Some aspect of our work must be discussed improving results understanding and also to introduce the pursuit of this research activities.

The use of the C-track system requires a referent frame calibration to measure the robot position. This frame is referenced using a manual touch probe. Experience has shown that

a bias is due to the use of this touch probe. Measurements can correct the positioning errors of the origin's frame, but do not correct its orientation errors. These residual defects affect our measurements and are visible in Section 4.1, when it is a matter of an observed bias (see Fig. 7). This gap is also present when comparing the measurements of the different checking fixtures. Using a more accurate measurement device should improve the benefits of the method, in particular by reducing the errors of offset of the base reference frame.

The major hypothesis of this study is that the stiffness behavior of the robot is linear since we assumed small robot displacements. However, we notice (Section 4.2) that the correction of the robot end-effector position is greater than 2 mm. The engagement of the tool in the material during the correction is therefore strongly modified, which leads to a significant modification of the cutting forces and the behavior of the robot, which may not respect the linearity hypothesis. One of the solutions will be to carry out an iteration of the method to validate this hypothesis in the context of small displacements. It is also planned to add a compensation based on a proportional analysis of the force since we experimentally

Fig. 15 ATOS and column measurement on Z before (4° path) and after (5° path) corrections

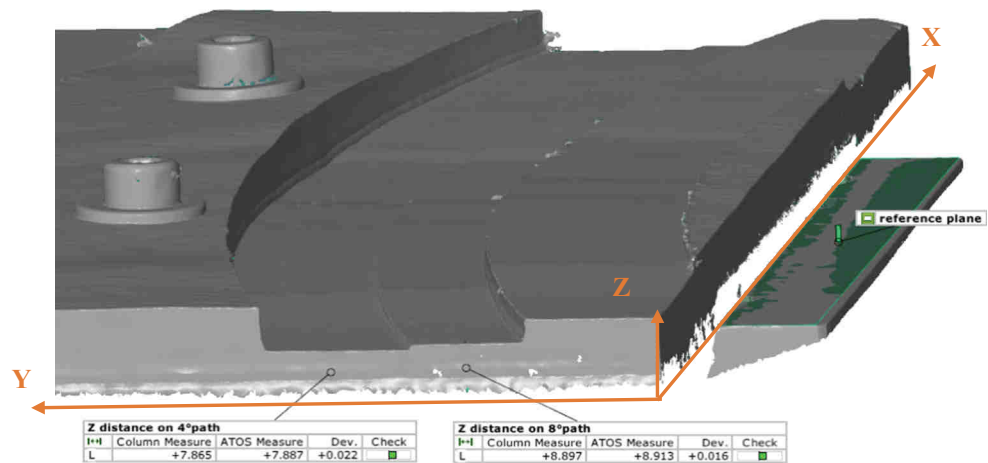


**Table 3** Workpiece measurements compared with measured deviation trajectory

Measurement mean	Before correction		After correction		Deviation	
	Y (mm)	Z (mm)	Y (mm)	Z (mm)	Y (mm)	Z (mm)
C-track	25.151	7.913	26.917	8.007	1.766	0.920
ATOS	22.738	7.887	20.946	8.913	1.792	1.026
HC3 column	22.714	7.865	20.920	8.897	1.794	1.032

approximate a proportionality between the robot displacement and the amplitude of the loads applied to the tool.

The off-line correction method detailed in this article does not allow to correct reversal defects that are directly related to mechanical play phenomena within the robot kinematic structure. Some dynamic characterizations such as in [7] conclude that generally the first three robot's joints are responsible for a major part of the inversion problems. Looking at the motion of the robot in the measurements made here, Figs. 10, 11, and 12, the Z axis motion is the cause of the observed inversion. In view of the configuration of the KUKA KR360 robot, the joints at fault are joints 2 and 3, since they are the ones most involved in the execution of the Z trajectory. In addition, they change the direction of rotation from Z+ to Z- and vice versa.

The studied trajectory does not allow an inspection along the X axis with ATOS and HC3 column devices. This limitation holds us to make statistically studies, it's why uncertainty on results is announced. New trajectories will be treated which will allow us to carry out a dimensional control on the three axes in order to present accurate results. The experimental deviation after correction is about  $0.329 \pm 0.109$  mm. In relation to the literature, Olabi et al. [30] had greater results with an addition of a stiffness correction, such as Cordes and Hintze [7] who denote a maximal deviation of 0.153 mm relative to a circular trajectory. This both studies are experimented on a small robot with stiffer structures. Schneider et al. [9] work on a robot similar to ours, and give a good relative deviation of  $\pm 0.1$  mm after coupling off-line and real-time correction. Regarding off-line compensation only, deviations are between 0.2 and 0.46 mm. Our results of about  $0.329 \pm 0.109$  mm of robot deviation after correction are relatively cloth. This article can easily be compared with all these cited works because of our much shorter characterization time, which allows our method to answer an industrial need on time and precision.

## 6 Conclusion

In this article, an off-line correction method suitable for robotic machining using an external position sensor is explored and applied. Inspired by mirror correction, the advantage of the method described resides in its application's speed and the

limitation of costs and means for its execution. This method improves positioning of the tool after measurement of a first machining operation. A treatment and analysis process are then applied to generate a compensated toolpath capable of reducing over 80% of the robot's initial measured deviations. A special feature of this off-line correction is its processing of the measured signal. It allows the use of a measuring device suitable for large amplitude measuring, in particular for production of large parts or for machining applications in an industrial environment.

This work has shown that the initial hypothesis, which is that the robot's deflection response is linear, is justified. However, the results showed that this same hypothesis is incomplete. This is because position correction changes the machining forces and the linearity of the robot response. To take it into account, iteration of the method for a second correction pass would reduce the average robot error. For this iteration, initial error would be a few tenths of a millimeter and the small displacement assumption would be obvious. Robot behavior, in a little position correction, would be minimized and results be much finer. Another perspective would be the use of a more accurate position sensor like a laser tracker to reduce the measurement precision.

## References

1. Muller C (2019) Welcome to the IFR press conference. Shanghai
2. Shiakolas PS, Conrad KI, Yih TC (2002) On the accuracy, repeatability, and degree of influence of kinematics parameters for industrial robots. *Int J Model Simul* 22(4):245–254
3. Dumas C, Boudelier A, Caro S, Garnier S, Ritou M, Furet B (2011) Development of a robotic cell for trimming composites. *Mecanique Ind* 12(6):487–494
4. Olabi A (2011) Improving the accuracy of industrial robots for high-speed machining applications, National higher school of arts and crafts
5. Belchior J, Guillo M, Courteille E, Maurine P, Leotoing L, Guines D (2013) Off-line compensation of the tool path deviations on robotic machining: application to incremental sheet forming. *Robot Comput Integr Manuf* 29(4):58–69
6. Gallot G, Dumas C, Garnier S, Caro S, Furet B (2012) Dynamic path correction for robotic processing, 13rd national conference aip primeca. (France)
7. Cordes M, Hintze W (2016) Offline simulation of path deviation due to joint compliance and hysteresis for robot machining. *Int J*



- Adv Manuf Technol 90:1075–1083. <https://doi.org/10.1007/s00170-016-9461-z>
8. Garnier S (2017) Identification and modelling for the development of machining monitoring and production robotics, phd thesis. (France)
  9. Schneider U, Drust M, Ansaloni M, Lehmann C, Pellicciari M, Leali F, Gunnink JW, Verl A (2016) Improving robotic machining accuracy through experimental error investigation and modular compensation. *The International Journal of Advanced Manufacturing Technology* 85:3–15
  10. Teti R (2002) Machining of composite materials. *CIRP Ann-Manuf Technol* 51:611–634
  11. Chibane H, Morandeau A, Serra R, Bouchou A, Leroy R (2013) Optimal milling conditions for carbon/epoxy composite material using damage and vibration analysis. *Int J Adv Manuf Technol* 68:1111–1121. <https://doi.org/10.1007/s00170-013-4903-3>
  12. Abrão AM, Rubio JCC, Faria PE, Davim JP (2008) The effect of cutting tool geometry on thrust force and delamination when drilling glass fibre reinforced plastic composite. *Mater Des* 29:508–513. <https://doi.org/10.1016/j.matdes.2007.01.016>
  13. Voß R, Henerichs M, Kuster F, Wegener K (2014) Chip root analysis after machining carbon fiber reinforced plastics (CFRP) at different fiber orientations. *Procedia CIRP* 14:217–222. <https://doi.org/10.1016/j.procir.2014.03.013>
  14. Pierre A (2013) Metrology: precision vs. accuracy, error vs. uncertainty. <https://aurelienpierre.com>
  15. Siciliano B, Kathib O (2008) *Handbook of robotics*, springer
  16. Schneider U, Ansaloni M, Drust M, Leali F, Verl A, (2013) Experimental investigation of sources of error in robot machining, *International Workshop on Robotics in Smart Manufacturing*. Springer, pp. 14–26
  17. Mustafa S.K, Pey Y.T, Yang G, Chen I (2010) A geometrical approach for online error compensation of industrial manipulator, *Proceedings of IEEE/ASME international conference on advanced intelligent mechatronics*, pp. 738–743 (montreal, Canada)
  18. Schneider U, Drust M, Diaz Posada J, Verl A (2013) Position control of an industrial robot using an optical measurement system for machining purposes
  19. Zhang H, Wang J, Zhang G, Gan Z, Pan Z, Cui H, Zhu Z (2005) Machining with flexible manipulator, Improving robotic machining performance. *IEEE*, pp. 1127–1132
  20. Pan Z, Zhang H, Zhu Z, Wang J (2006) Chatter analysis of robotic machining process. *J Mater Process Technol* 173(3):301–309
  21. Chen T, Xiang J, Gao F, Liu X, Liu G (2019) Study on cutting performance of diamond-coated rhombic milling cutter in machining carbon fiber composites. *Int J Adv Manuf Technol* 103(9-12): 4731–4737
  22. Tankus K, Tascioglu E, Atay G, Brunken H, Kaynak Y (2020) The effect of cutting parameters and cutting tools on machining performance of carbon graphite material. *Mach Sci Technol* 24:96–111. <https://doi.org/10.1080/10910344.2019.1701020>
  23. Henerichs M, Voß R, Kuster F, Wegener K (2015) Machining of carbon fiber reinforced plastics: Influence of tool geometry and fiber orientation on the machining forces. *CIRP J Manuf Sci Technol* 9:136–145. <https://doi.org/10.1016/j.cirpj.2014.11.002>
  24. NF E66-520-1 (1997) Operating range of cutting tools - tool-material pair
  25. Creaform brochure. [www.creaform3d.com/sites/default/files/assets/brochures/files/fr-vxtrack\\_feuille\\_fr\\_11122018](http://www.creaform3d.com/sites/default/files/assets/brochures/files/fr-vxtrack_feuille_fr_11122018)
  26. Atos brochure. [www.cetimsudouest.fr/technologies-moyens/optique](http://www.cetimsudouest.fr/technologies-moyens/optique)
  27. Sheikh-Ahmad JY (2009) *Machining of polymer composites*. Springer, New York
  28. Gaitonde VN, Karnik SR, Rubio JC, Correia AE, Abrão AM, Davim JP (2008) Analysis of parametric influence on delamination in high-speed drilling of carbon fiber reinforced plastic composites. *J Mater Process Technol* 203:431–438. <https://doi.org/10.1016/j.jmatprotec.2007.10.050>
  29. Morandeau A, Leroy R, Bouchou A, Bonhoure D (2011) Usinage des composites renforcés en fibres de carbone: stratégie de surfacage pour limiter les efforts de coupe, 17th National Composites Days (JNC17). p. 126
  30. Olabi A, Damak M, Bearee R, Gibaru O, Leleu S (2012) Improving the accuracy of industrial robots by offline compensation of joints errors. In: *Industrial Technology (ICIT), 2012 IEEE International Conference On*. IEEE, pp. 492–497.
  31. Lei WT, Sung MP (2008) Nurbs-based fast geometric error compensation for cnc machine tools. *Int J Mach Tools Manuf* 48(3-4): 307–319
  32. Guiassa R (2012) *Methods of compensating for machining errors using measurement on machine tools*, Phd thesis, Polytechnique school of Montreal
  33. Shen H, Fu J, He Y, Yao X (2012) On-line asynchronous compensation methods for static/quasi-static error implemented on cnc machine tools. *Int J Mach Tools Manuf* 60:14–26
  34. Thiery C, Scherrer B (2010) Least-Squares  $\lambda$  Policy Iteration: optimism and bias-variance trade-off for optimal control, 26
  35. Duan H, Zhang R, Yu F, Gao J, Chen Y (2016) Optimal trajectory planning for glass-handing robot based on execution time acceleration and jerk. *J Robot* 2016:1–9. <https://doi.org/10.1155/2016/9329131>